Robotics and Autonomous Systems 98 (2017) 56–66

Contents lists available at ScienceDirect

Robotics and Autonomous Systems

journal homepage: www.elsevier.com/locate/robot

Geometrical/analytical approach for reciprocal screw-based singularity analysis of a novel dexterous minimally invasive manipulator

Alaa Khalifa *, Mohamed Fanni [1], Abdelfatah M. Mohamed [2]

Mechatronics and Robotics Engineering Department, Egypt-Japan University of Science and Technology, E-JUST, New Borg El-Arab City, Alexandria, Egypt

ARTICLE INFO

Article history:
Received 28 August 2016
Received in revised form 5 August 2017
Accepted 5 September 2017
Available online 20 September 2017

Keywords:
Minimally Invasive Surgery
Dexterous instrument
Parallel manipulator
Reciprocal screws
Constraint singularity
Architecture singularity

ABSTRACT

This paper is concerned with the singularity analysis of a novel 4-DOF endoscopic surgical parallel manipulator (2-PUU_2-PUS). This parallel manipulator has larger bending angles compared to previously existing surgical parallel manipulators. It is easy to imagine the singular configurations inside the workspace of a manipulator with a zero pitch and infinity pitch reciprocal screws. On the other hand, the (2-PUU_2-PUS) surgical manipulator has two reciprocal screws of h-pitch. Hence, the singular configurations of this manipulator could not be provided by the known reciprocal screw-based geometrical approach. Therefore, the geometrical/analytical approach for reciprocal screw-based singularity analysis of 2-PUU_2-PUS is proposed in this work. The results illustrate the feasibility of the proposed algorithm to find all singular configurations of the 2-PUU_2-PUS manipulator. The discovered singularity configurations greatly shrink the singularity-free workspace to be one-fourth of the original workspace. In order to be able to work through the entire workspace, we suggest changing the topology structure of the manipulator.

© 2017 Elsevier B.V. All rights reserved.

1. Introduction

Recently, surgical procedures have become less invasive. Minimally Invasive Surgery (MIS) becomes more and more applicable in therapeutic uses. Open surgical approaches require many procedures that increase the difficulty of the process. MIS has replaced these open approaches because it requires a small number of surgical procedures. MIS also has many benefits, so it is becoming the new standard in medicine. These benefits include improving the aesthetics and reduction in recovery time in the hospital.

In general, clinical endoscopic manipulators are categorized into two main types: serial mechanism and rigid mechanism manipulators. Serial mechanisms are used in the majority of commercial surgical systems. These mechanisms rely on the wires to transfer the mechanical movement [1]. Commercial systems that use serial mechanisms are presented in two types. The first one is the da Vinci system produced by Intuitive Surgical, Inc. [2] and this is the one in clinical use currently. The second one is the Zeus system produced by computer motion, Inc. [3] and this one is no longer in clinical use.

Ulrich et al. [4] presented MiroSurge, a setup of the Miro-robotic surgery platform (MRSP), which enables bi-manual endoscopic telesurgery. The MRSP is an extensible and configurable platform that is anticipated to achieve the dedicated requirements of different surgical applications. Inside the patient's body, the MICA instruments act as working end effectors, consequently enhancing the dexterity of the robot behind the skin barrier. These MICA instruments consist of a long shaft, functional tip, and driving unit. In the MICA instrument, the functional tip contains a universal joint that is driven by wires to increase the level of dexterity. A snake-like device with multi-backbone was introduced in [5]. This instrument has a diameter of 4.2 mm and possesses a bending angle of $\pm 90^\circ$ in all directions. The bending process depends on three superelastic wires for performing pull and push modes. The force analysis of the instrument is investigated in [6]. However, large bending force and rigidity are not expected.

The design and analysis of an articulating drive instrument for endoscopic surgery were presented by Wei et al. [7]. In spite of limitations in size of the first generation, the design has been successfully proven to be used in the second iteration. A new orientation robot, with a modular structure, intended for MIS instruments was proposed in [8]. The main drawback which is reported for this robot is the usage of wires for bending. A new plastic wrist for MIS was

* Corresponding author.
E-mail address: alaa.khalifa@ejust.edu.eg (A. Khalifa).
[1] On leave from Production Engineering and Mechanical Design Department, Faculty of Engineering, Mansoura University, Egypt.
[2] On leave from Electrical Engineering Department, Faculty of Engineering, Assiut University, Egypt.

http://dx.doi.org/10.1016/j.robot.2017.09.005
0921-8890/© 2017 Elsevier B.V. All rights reserved.

introduced in [9]. This wrist is compact and disposable (to avoid nosocomial contaminations) and contains free space for different connections like NiTi wires, fluidic tubes, and fiber optics. The mechanical structure of the wrist utilizes 0.3 mm NiTi superelastic wires for bending which allows two DOF.

However, the use of the wire-actuated type is widely spread out; it has many flaws such as difficulty in the process of sterilization in endoscopic applications. Also, rupture of the wire may occur during the operation, and the surgeon needs to complete the operation by himself. Furthermore, cable-driven mechanics suffer from a type of wire actuation and can be transferred only by tugging. Moreover, wires may be slack, and it is required to design a mechanism to pre-tension the wires. In order to avoid these problems, it is proposed to use a rigid mechanism as the slave manipulator.

The second type is the rigid mechanism manipulator which uses a parallel manipulator in the process of transmitting the motion to the end effector and performs the surgery. Recently, parallel mechanisms are actively participating in many medical applications because of their potential advantages compared with those of the serial. These advantages are large payload capacity, high structural stiffness, accurate positioning, and easiness of the sterilization process.

An active hybrid parallel robot for MIS was presented in [10]. Also, the kinematic and dynamic behavior of this hybrid parallel robot is investigated. The robot is comprised of two subsystems: a surgical arm, PARASURG 5M with five actuators, and an active surgical instrument PARASIM with four actuators. The ranges of the orientation angles are very limited which is a significant defect in surgical applications. Elastostatic model for a novel hybrid robot for MIS was introduced in [11]. The parallel manipulator has two similar chains of SPU sort and an RRR chain, which enables the end-effector to achieve spherical movement. The robot possesses three active joints for the parallel manipulator and one for the translational movement along the axis of the surgical tool. However, the bending angle of this novel robot could not exceed $\pm 60^\circ$ in any direction.

A 4-DOF parallel manipulator (2-PUU_2-PUS) was proposed in [12]. The feasibility of (2-PUU_2-PUS) design is proved by computer simulations. The bending angle of this manipulator reached $\pm 90^\circ$ in all directions. A real model of the 4-DOF parallel manipulator is fabricated from annealed stainless steel. It is found during experimental work that the movable platform of the proposed parallel manipulator could not resist forces in some configurations. Hence, a thorough singularity analysis is needed to discover the source of the above problem. Also, design modification of the proposed manipulator is necessary to overcome this problem. The main goal of this research is to investigate the singularity problems and determine all the singular points inside the workspace.

One of the core issues of a parallel manipulator is the singularity analysis. Unlike serial manipulators that lose degrees of freedom in the singular configuration, parallel manipulators may also earn degrees of freedom although the actuators are locked. This acquisition of degrees of freedom is called parallel singularities, resulting in unstable or uncontrollable configurations [13].

One of the main methods used for finding the singular configurations of parallel manipulators depends on the computation of the Jacobian determinant degeneracy. In general, the Jacobian matrix expresses a system of screws. The determinant of this Jacobian matrix is highly nonlinear and impractical to assess for the majority of the manipulators. Therefore, satisfactory results could not be obtained using linear algebra. Thus, the use of geometrical approaches such as Grassmann Geometry (GG) [14] and Grassmann–Cayley Algebra (GCA) [15] is introduced. Line geometry is used to consider dependency of the wrenches of actuated joints to find singular configurations by Notash [16] and Dash et al. [17]. The singular configurations of a 6-DOF parallel manipulator are studied by Merlet [18]. During this study, a geometric method is utilized instead of determining roots of the determinants of the Jacobian matrix. A general approach to locating the singularities of any mechanism with arbitrary chains and an equal number of outputs and inputs was introduced by Zlatanov et al. [19]. They determined the singular configurations using a velocity equation which includes the velocities of passive and active joints.

An approach for the inverse Jacobian of limited-DOF parallel manipulators was developed by Joshi and Tsai [20]. This methodology is based on the theory of reciprocal screws to determine a (6×6) inverse Jacobian matrix. The rows of this matrix are actuation and constraint wrenches applied to the movable platform. These wrenches, known as governing lines, provide information about both constraint and architecture singularities.

All previous manipulators have a zero pitch and infinity pitch reciprocal screws, so it is easy to imagine the singular configurations inside the workspace. A zero pitch reciprocal screw means that the movable platform is constrained by a pure force. Furthermore, an infinity pitch reciprocal screw means that the movable platform is constrained by a pure couple. On the other hand, the novel 4-DOF surgical manipulator (2-PUU_2-PUS) has two h-pitch reciprocal screws. The reciprocal screw of h-pitch means that the movable platform is constrained by a combination of forces and couples that have a certain relationship. It is difficult to find out the singular configurations geometrically in such cases since h-pitch reciprocal screw changes its pitch value with a change in its configuration. Geometrical/Analytical approach for reciprocal screw-based singularity analysis of 2-PUU_2-PUS is proposed in this work. The proposed algorithm can find all singular configurations of any limited DOF parallel manipulator with h-pitch reciprocal screws. The proposed algorithm will be discussed in details in this paper.

This paper is organized as follows. In Section 2, the description of the slave surgical manipulator is briefly presented. Jacobian analysis of a parallel manipulator with limited-DOF is discussed in Section 3. The proposed geometrical/analytical approach for reciprocal screw-based singularity analysis of 2-PUU_2-PUS is provided in Section 4. In Section 5, singular configurations of the parallel surgical manipulator (2-PUU_2-PUS) are described. Finally, conclusions and future work are summarized in Section 6.

2. Slave manipulator description

Teleoperation system enables the surgeon to remotely control a slave manipulator, which interacts with the environment and performs the required task, by the movement of another robot called the master device. Our practical implementation of the whole teleoperation system uses the new endoscopic parallel manipulator (2-PUU_2-PUS) for laparoscopic surgery as the slave manipulator and PHANTOM-Omni haptic device as the master robot. Generally, the parallel manipulator (2-PUU_2-PUS) will be used as an endoscopic manipulator for MIS. Our work gives extra focus on the liver surgeries.

2-PUU_2-PUS architecture is the implemented design of the slave surgical manipulator. The schematic diagram of the proposed endoscopic surgical manipulator (2-PUU_2-PUS) is shown in Fig. 1. To obtain larger bending angles and workspace volume, the design of the 4-DOF parallel manipulator (2-PUU_2-PUS) is performed using parallel virtual chain methodology and the screw theory. This parallel manipulator consists of four limbs; two limbs are 2-PUU (each limb contains one active prismatic joint and two consecutive passive universal joints, respectively); the other two limbs are 2-PUS (each limb contains one active prismatic joint, one passive universal joint, and one passive spherical joint, respectively). The base platform is connected to each limb by the active prismatic (P) joint. The bending angles are the same in all directions due to symmetry in the manipulator design.

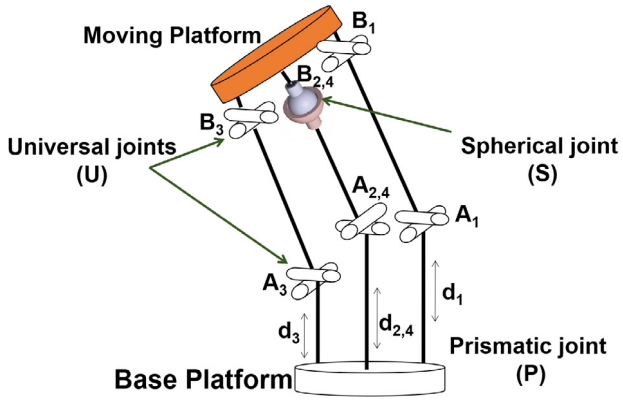

Fig. 1. Schematic diagram of 4-DOF parallel manipulator (2-PUU_2-PUS).

Fig. 2. Real model of the proposed endoscopic surgical manipulator.

The real prototype of the designed endoscopic surgical manipulator (2-PUU_2-PUS) is fabricated from annealed stainless steel as illustrated in Fig. 2. For some considerations in the manufacturing process for this small scale, the spherical joint is implemented through the use of one universal joint followed by one revolute joint whose axis is orthogonal to the two axes of the universal joint and intersect with them at one point.

The 2-PUU_2-PUS manipulator will be attached to a holder unit, which is clamped to a rigid frame above the patient. This holder unit is used for positioning the proposed manipulator (2-PUU_2-PUS) inside the patient's body and providing any required coarse motion. A surgical tool (scissors, grippers, optics, etc.) will be rigidly attached to the movable platform by fixation screw. Moreover, a central hole is made in the fixed base platform, as well as in the movable platform, for permitting any wiring connection needed for the surgical tool.

For load simulation, the proposed manipulator (2-PUU_2-PUS) is in a straight configuration with locked prismatic joints. In addition, a force of 5 N is applied vertically in the Z-direction to the movable platform. In this case, the maximum stress is less than 30 MPa, which is far away from the yield point of the manipulator's material (275 MPa). Additionally, the maximum observed deflection is very small and within the acceptable boundaries [12].

3. Jacobian analysis of a parallel manipulator with limited-DOF

Tsai et al. [20] used the reciprocal screws to build an overall square Jacobian matrix (6×6) for any parallel manipulator with limited DOF. This generalized Jacobian matrix will be discussed briefly in this section. A limited DOF parallel manipulator has F-DOF, considering F is between 0 and 6. Furthermore, F limbs constrained the movable platform. It is considered that only one actuator drives each limb as we are interested in this case only. The reciprocal screw theory is applied to find the Jacobian matrix that relates the joints rate and the end-effector velocities. Overall Jacobian matrix gives information about both constraint and architecture singularities. Constraint singularities arise when the limbs of a parallel manipulator lose their ability to constrain the movable platform to move with the intended motion. On the other hand, architecture singularities refer to the conditions for which the actuators cannot control the linear velocity of the movable platform.

We can express both finite and infinitesimal motions of any rigid body by a rotation about a particular axis and a translation along the same axis [21]. This unique axis is known as a screw axis. Moreover, the combined motion is known as a twist. The pitch of the screw (λ) is the ratio of translation to the rotation. A unit screw can be identified by a unit vector along the screw axis (s) and the position vector for any point located at the screw axis (s_0). A similar concept can be realized for statics, a system of forces and couples acting on any rigid body can be expressed as a resultant force acting along a unique axis and a resultant couple about the same axis. This combination of force and couple is called a reciprocal screw (wrench). The ratio of the couple to the force is called the pitch of the reciprocal screw.

The connectivity, C_i, of a limb is defined as the number of degrees of freedom associated with all the joints existing in the ith limb. A spherical joint can be replaced by three intersecting non-coplanar revolute joints. The universal joint can be replaced by two intersecting revolute joints. The ith limb may be considered as a serial chain connecting the movable platform to the fixed base by a C_i number of 1-DOF joints. According to the above considerations, the instantaneous twist of the movable platform, $\$_p$, can be expressed as a linear combination of the instantaneous twist of all joints in the limb:

$$\$_p = \sum_{j=1}^{C_i} \dot{\theta}_{j,i} \cdot \hat{\$}_{j,i} \qquad \text{for } i = 1, 2, \ldots, F, \tag{1}$$

where $\dot{\theta}_{j,i}$ symbolizes the rate of the jth joint in the ith limb. Also, $\hat{\$}_{j,i}$ denotes a unit screw along the axis of the jth joint in the ith limb. The instantaneous twist of the movable platform is found to be $\$_p = \left[\omega^T, v_p^T\right]^T$, where ω is the angular velocity of the movable platform and v_p is the linear velocity of a point which is embedded in the movable platform and instantaneously coincident with the origin of the reference frame at which the screws are expressed.

– Jacobian of constraints

The screws, which are reciprocal to all the joint screws as well as active and passive joints of the ith limb, form a $(6 - C_i)$ reciprocal basis screw system. The kth reciprocal screw of the ith limb can be represented as $\hat{\$}_{r,k,i}$. Performing the orthogonal product to both sides of Eq. (1) with each reciprocal basis screw produces:

$$\hat{\$}_{r,k,i}^T \cdot \$_p = 0 \qquad \text{for } k = 1, 2, \ldots, (6 - C_i). \tag{2}$$

This equation is written once for each limb to yield $\sum_{i=1}^{F}(6 - C_i)$ equations that can be written in matrix form as:

$$J_c \cdot \$_p = 0, \tag{3}$$

where J_c is the Jacobian of constraints matrix. A unit wrench of constraints imposed by the joints of a limb will be represented as a row in the Jacobian of constraint matrix, J_c. The rank of J_c must be equal to (6-F) to properly constrain the movable platform to the intended F-DOF motion.

– Jacobian of Actuators

Now, the active joint in each limb will be locked. The dimension of the reciprocal screws will increase by one. The screws which are reciprocal to all the passive joint screws form a $(6 - C_i + 1)$ reciprocal screw system. In this regard, we represent the reciprocal basis screw as $\hat{\$}_{r,6-C_i+1,i}$. Considering the case in which the first joint in the ith limb is the active one, performing the orthogonal product to both sides of Eq. (1) with $\hat{\$}_{r,6-C_i+1,i}$ will produce:

$$\hat{\$}^T_{r,6-C_i+1,i} \cdot \$_p = \dot{\theta}_{1,i} \cdot \hat{\$}^T_{r,6-C_i+1,i} \cdot \hat{\$}_{1,i} \,. \tag{4}$$

F equations can be obtained by writing the previous equation once for each limb. These F equations can be written in matrix form as:

$$J_x \cdot \$_p = J_q \cdot \dot{q}, \tag{5}$$

where $\dot{q}$ is an $F \times 1$ vector that represents the active joints' rates $(\dot{\theta}_{1,i})$. J_x is an $F \times 6$ matrix and J_q is an $F \times F$ diagonal matrix. Multiplying both sides of the equation by the diagonal matrix J_q^{-1} yields:

$$\dot{q} = J_a \cdot \$_p, \tag{6}$$

where J_a is called the Jacobian of actuation matrix and its dimension is $F \times 6$. J_a should have a full rank i.e. its rank equals to F.

– Overall Jacobian

If we complement the Jacobian of constraints with the Jacobian of actuators, we will obtain:

$$\dot{q_o} = J \cdot \$_p, \tag{7}$$

where $\dot{q_o} = \begin{bmatrix} \dot{q}_{F\times 1} \\ 0_{(6-F)\times 1} \end{bmatrix}$, and $J = \begin{bmatrix} J_a \\ J_c \end{bmatrix}$. $\dot{q_o}$ is a 6×1 vector and J is the overall Jacobian of the limited DOF parallel manipulator. J is a 6×6 matrix which is developed to fully characterize the instantaneous movement of the movable platform. This 6×6 overall Jacobian matrix is obtained although F is less than six. The upper $F \times 6$ sub-matrix of the overall Jacobian relates the angular and linear velocities of the movable platform to the active joints' rates. On the other hand, the lower $(6 - F) \times 6$ sub-matrix of the overall Jacobian constrains the movable platform to F-DOF instantaneous motion. When J_c loses its rank, constraint singularity will occur. Moreover, when det(J) = 0 but J_c has a full rank, architecture singularity will occur.

4. Proposed geometrical/analytical approach for reciprocal screw-based singularity analysis of 2-PUU_2-PUS

Fig. 3 shows the schematic representation of the first limb and its joints' axes. Points O and C refer to the center of the fixed base platform and the movable platform, respectively. The intersection between the prismatic joint and the fixed base is represented as P_i (*for* $i = 1, 2, 3, 4$). Points P_i are symmetrically arranged in a perimeter of a circle with radius R. Points A_i (*for* $i = 1, 2, 3, 4$) denote the location of the first universal joint in the ith limb. Points B_i (*for* $i = 1, 3$) represent the location of the second universal joint in the ith limb, whereas points B_i (*for* $i = 2, 4$) denote the location of the spherical joint in the ith limb. A fixed frame O-XYZ is attached to the center of the fixed plate in which the X-axis points to the direction of OP_1. Moreover, the Z-axis is perpendicular to the plane of the base plate. Finally, the Y-axis will satisfy the right-hand rule. Furthermore, at the center of the mobile plate, a mobile frame C-UVW with the same pose as the fixed frame is attached. Considering the first limb PUU, those fixed and mobile frames are shown in Fig. 3. The P-joint that connects the base plate to the limb is the active joint. Due to the movement of the actuators, links P_iA_i are of variable lengths d_i in the Z-direction. Links P_iA_i and A_iB_i are tied by the universal joint. Links A_iB_i are of fixed length L_i.

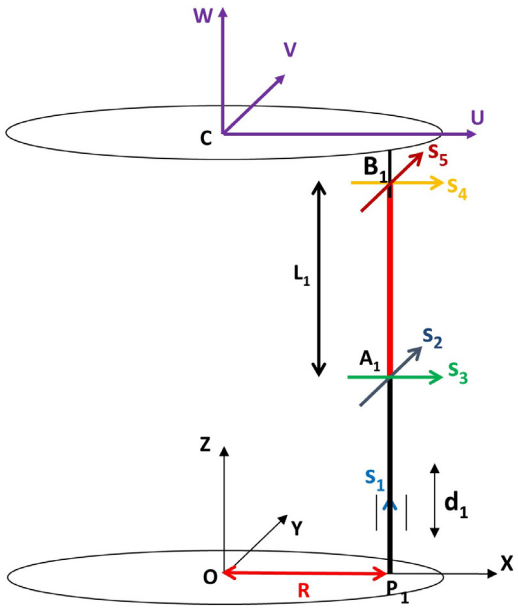

Fig. 3. Schematic representation of first chain PUU.

The coordinates of the points P_i referred to the fixed base reference frame XYZ are given by:

$$P_1 = \begin{bmatrix} R \\ 0 \\ 0 \end{bmatrix}, \quad P_2 = \begin{bmatrix} 0 \\ R \\ 0 \end{bmatrix}, \quad P_3 = \begin{bmatrix} -R \\ 0 \\ 0 \end{bmatrix}, \quad P_4 = \begin{bmatrix} 0 \\ -R \\ 0 \end{bmatrix}. \tag{8}$$

While the coordinates of points A_i can be calculated from:

$$A_i = P_i + \begin{bmatrix} 0 \\ 0 \\ d_i \end{bmatrix} \qquad \textit{for } i = 1, 2, 3, 4. \tag{9}$$

In the following subsections, we will calculate the unit screw associated with all joints' axes in each limb of the manipulator. Then, we will find the reciprocal screws with the actuators locked and without locking the actuators. We make these calculations for each limb individually.

4.1. First and third limbs

Each limb of the first and third limbs connects the fixed plate to the movable platform by a prismatic joint followed by two universal joints (PUU) as illustrated in Fig. 3. The prismatic joint is driven by a linear actuator. In this section, the position vector of the second universal joint B_i ($i = 1, 3$ for first and third limb, respectively) with respect to O-XYZ can be described as:

$$B_i = A_i + rot_y(\alpha_i) \cdot rot_x(\beta_i) \cdot \begin{bmatrix} 0 \\ 0 \\ L_i \end{bmatrix} = \begin{bmatrix} \psi + L_i \sin(\alpha_i)\cos(\beta_i) \\ -L_i \sin(\beta_i) \\ d_i + L_i \cos(\alpha_i)\cos(\beta_i) \end{bmatrix}, \tag{10}$$

where α_i and β_i are the two angles of the first universal joint in the ith limb (*for* $i = 1, 3$). Also, $rot_{(*)}$ is a rotation matrix representing

a rotation of angle(*) about axis(.). See [21] for the definition of the rotation matrix. For the easy flow of equations, we use $\psi = R$ for the first limb ($i = 1$) and $\psi = -R$ for the third limb ($i = 3$).

Let $s_{j,i}$ be a unit vector along the jth joint axis of the ith limb (*for* $i = 1, 3$; *and* $j = 1, 2, \ldots, 5$). Now, we will calculate the unit vector associated with all joints' axes in the first and third limbs. The fixed frame O-XYZ is chosen to be the reference frame at which all the screws are expressed.

$$s_{1,i} = \begin{bmatrix} 0 \\ 0 \\ 1 \end{bmatrix}, \qquad s_{2,i} = \begin{bmatrix} 0 \\ 1 \\ 0 \end{bmatrix}, \tag{11}$$

$$s_{3,i} = rot_y(\alpha_i) \cdot \begin{bmatrix} 1 \\ 0 \\ 0 \end{bmatrix} = \begin{bmatrix} \cos(\alpha_i) \\ 0 \\ -\sin(\alpha_i) \end{bmatrix}, \tag{12}$$

$$s_{4,i} = rot_y(\alpha_i) \cdot rot_x(\beta_i) \cdot \begin{bmatrix} 1 \\ 0 \\ 0 \end{bmatrix} = \begin{bmatrix} \cos(\alpha_i) \\ 0 \\ -\sin(\alpha_i) \end{bmatrix}, \tag{13}$$

$$\begin{aligned} s_{5,i} &= rot_y(\alpha_i) \cdot rot_x(\beta_i) \cdot rot_x(\gamma_i) \cdot \begin{bmatrix} 0 \\ 1 \\ 0 \end{bmatrix} \\ &= \begin{bmatrix} \sin(\alpha_i)\sin(\beta_i + \gamma_i) \\ \cos(\beta_i + \gamma_i) \\ \cos(\alpha_i)\sin(\beta_i + \gamma_i) \end{bmatrix}, \end{aligned} \tag{14}$$

where γ_i and δ_i are the two angles of the second universal joint in the ith limb (*for* $i = 1, 3$). For the prismatic joint, the pitch of the screw will be infinity and the unit screw is reduced to:

$$\hat{\$}_{1,i} = \begin{bmatrix} [0]_{3\times1} \\ s_{1,i} \end{bmatrix} \qquad for\ i = 1, 3. \tag{15}$$

As mentioned before, the universal joint can be replaced by two intersecting revolute joints. For the revolute joint, the pitch of the screw will be zero and the unit screw is calculated as:

$$\hat{\$}_{k,i} = \begin{bmatrix} s_{k,i} \\ s_{0k,i} \times s_{k,i} \end{bmatrix} \qquad for\ k = 2, 3, 4, 5. \tag{16}$$

Moreover, $s_{0k,i}$ is the position vector of a point existing on the screw axis and it is found to be:

$$s_{0k,i} = \begin{cases} A_i & for\ k = 2, 3. \\ B_i & for\ k = 4, 5. \end{cases} \tag{17}$$

With the actuator locked, the connectivity of each limb of the first and third limbs is equal to 4. The reciprocal screws, which are reciprocal to all the passive joints' screws in the ith limb, form a 2-system. One screw, $\hat{\$}_{r1,i}$, can be readily identified as a zero pitch screw along the line passing through the two centers of the two universal joints that existed in the ith limb. The second screw, $\hat{\$}_{r2,i}$, which is also reciprocal to all the passive joint screws, can be readily identified as a zero pitch screw along the intersection line between two planes as shown in Fig. 4. The first plane contains the two axes of the first universal joint and the second plane contains the two axes of the second universal joint.

Let $s_{r1,i}$ be a unit vector along the line passing through the two centers of the two universal joints in the ith limb. $s_{r1,i}$ can be identified easily from:

$$s_{r1,i} = rot_y(\alpha_i) \cdot rot_x(\beta_i) \cdot \begin{bmatrix} 0 \\ 0 \\ 1 \end{bmatrix} = \begin{bmatrix} \sin(\alpha_i)\cos(\beta_i) \\ -\sin(\beta_i) \\ \cos(\alpha_i)\cos(\beta_i) \end{bmatrix}. \tag{18}$$

Furthermore, $s_{r01,i}$ is a vector from the reference frame to a point that existed on the line passing through the two centers of the two universal joints, which easily can be calculated from:

$$s_{r01,i} = A_i \qquad for\ i = 1, 3. \tag{19}$$

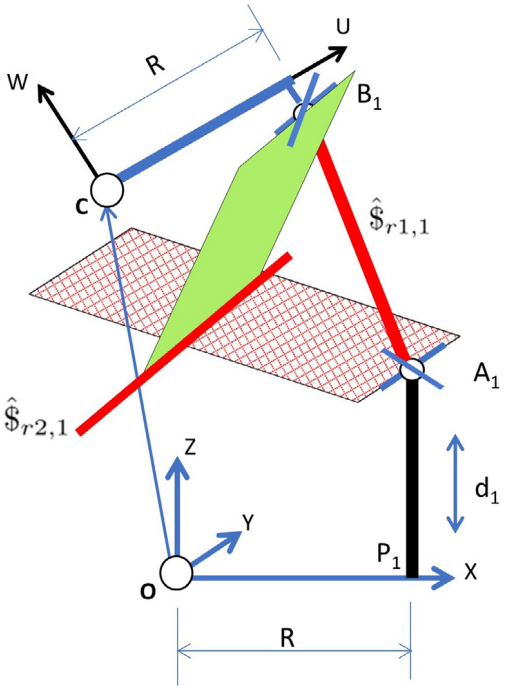

Fig. 4. Reciprocal screws of first chain PUU.

Knowing $s_{r1,i}$ and $s_{r01,i}$, we can identify a zero pitch screw, $\hat{\$}_{r1,i}$, according to:

$$\hat{\$}_{r1,i} = \begin{bmatrix} \sin(\alpha_i)\cos(\beta_i) \\ -\sin(\beta_i) \\ \cos(\alpha_i)\cos(\beta_i) \\ d_i \sin(\beta_i) \\ d_i \sin(\alpha_i)\cos(\beta_i) - \psi\cos(\alpha_i)\cos(\beta_i) \\ -\psi\sin(\beta_i) \end{bmatrix}. \tag{20}$$

In order to find the equation of the first plane, which contains the two axes of the first universal joint, we must specify a point on the plane and a vector that is orthogonal to the plane. This orthogonal vector is called the normal vector $n_{1,i}$ which can be identified as:

$$n_{1,i} = s_{2,i} \times s_{3,i} = \begin{bmatrix} -\sin(\alpha_i) \\ 0 \\ -\cos(\alpha_i) \end{bmatrix}. \tag{21}$$

Also, we can take A_i as the point that lies on the plane. Then, the equation of the plane can be expressed as:

$$-\sin(\alpha_i)X - \cos(\alpha_i)Z = dp_{1,i}\ , \tag{22}$$

where $dp_{1,i} = n_{1,i}^T \cdot A_i = -\psi\sin(\alpha_i) - d_i\cos(\alpha_i)$.

Concerning the equation of the second plane which contains the two axes of the second universal joint, we must specify a point on the plane and the normal vector $n_{2,i}$. This normal vector $n_{2,i}$ can be identified as:

$$n_{2,i} = s_{4,i} \times s_{5,i} = \begin{bmatrix} \sin(\alpha_i)\cos(\beta_i + \gamma_i) \\ -\sin(\beta_i + \gamma_i) \\ \cos(\alpha_i)\cos(\beta_i + \gamma_i) \end{bmatrix}. \tag{23}$$

Moreover, we can consider B_i as the point that lies on the second plane. Then, the equation of the plane can be expressed as:

$$\begin{aligned} &\sin(\alpha_i)\cos(\beta_i + \gamma_i)X - \sin(\beta_i + \gamma_i)Y + \cos(\alpha_i)\cos(\beta_i + \gamma_i)Z \\ &\quad = dp_{2,i}\ , \end{aligned} \tag{24}$$

where $dp_{2,i} = n_{2,i}^T \cdot B_i = L_i \sin(\beta_i + \gamma_i)\sin(\beta_i) + \cos(\beta_i + \gamma_i)\cos(\alpha_i)[d_i + L_i\cos(\alpha_i)\cos(\beta_i)] + \cos(\beta_i + \gamma_i)\sin(\alpha_i)[\psi + L_i\sin(\alpha_i)\cos(\beta_i)]$.

The intersection line between the two planes is orthogonal to the normal vector $n_{1,i}$ of the first plane and the normal vector $n_{2,i}$ of the second plane. This intersection line V_i can be recognized from:

$$V_i = n_{1,i} \times n_{2,i} = \begin{bmatrix} -\cos(\alpha_i)\sin(\beta_i + \gamma_i) \\ 0 \\ \sin(\alpha_i)\sin(\beta_i + \gamma_i) \end{bmatrix}. \tag{25}$$

$$s_{r2,i} = \frac{V_i}{\|V_i\|} = \begin{bmatrix} -\cos(\alpha_i) \\ 0 \\ \sin(\alpha_i) \end{bmatrix}, \tag{26}$$

where $s_{r2,i}$ is a unit vector that lies on the intersection line between the two planes, the first plane contains the two axes of the first universal joint and the second plane contains the two axes of the second universal joint.

In order to completely identify the second screw, $\hat{\$}_{r2,i}$, we also need to find a point located on the two planes. By solving the two equations of the two planes, we found that:

$$s_{r02,i} = \begin{bmatrix} \dfrac{dp_{1,i}}{-\sin(\alpha_i)} \\ \dfrac{dp_{2,i} + \cos(\beta_i + \gamma_i)dp_{1,i}}{-\sin(\beta_i + \gamma_i)} \\ 0 \end{bmatrix}, \tag{27}$$

where $s_{r02,i}$ is a vector from the origin of the reference frame to any point on the intersection line between the two planes. The second reciprocal screw, $\hat{\$}_{r2,i}$, can be identified as a zero pitch screw along the intersection line between the two planes and calculated according to:

$$\hat{\$}_{r2,i} = \begin{bmatrix} -\cos(\alpha_i) \\ 0 \\ \sin(\alpha_i) \\ -L_i\sin(\alpha_i)\cos(\gamma_i)/\sin(\beta_i + \gamma_i) \\ -d_i\cos(\alpha_i) - \psi\sin(\alpha_i) \\ -L_i\cos(\alpha_i)\cos(\gamma_i)/\sin(\beta_i + \gamma_i) \end{bmatrix}. \tag{28}$$

Without locking the prismatic joint, the connectivity is equal to 5 for each limb of first and third limbs. Hence, the reciprocal screws for each limb form a 1-system which is a screw that is reciprocal to all the joint screws of the ith limb. This reciprocal screw, $\hat{\$}_{rt,i}$, is a linear combination between $\hat{\$}_{r1,i}$ and $\hat{\$}_{r2,i}$ which must satisfy the condition to be reciprocal with the prismatic joint screw. This linear combination is illustrated as:

$$\frac{a_i}{\sqrt{a_i^2 + b_i^2}}\hat{\$}_{r1,i} + \frac{b_i}{\sqrt{a_i^2 + b_i^2}}\hat{\$}_{r2,i} = \hat{\$}_{rt,i}\ , \tag{29}$$

where a_i and b_i are unknown numbers which satisfy the equation. In the above linear combination, we divided by $\sqrt{a_i^2 + b_i^2}$ to get a unit reciprocal screw. Furthermore, we know the general form of the reciprocal screw which is expressed as:

$$\hat{\$}_{rt,i} = \begin{bmatrix} s_{rt,i} \\ s_{0rt,i} \times s_{rt,i} + \lambda_i \cdot s_{rt,i} \end{bmatrix}, \tag{30}$$

where $s_{rt,i}$ is a unit vector along the axis of the reciprocal screw $\hat{\$}_{rt,i}$, which is reciprocal to all the joint screws of the ith limb. Also, $s_{0rt,i}$ refers to the vector from the origin of the reference frame to any point that existed on the axis of the reciprocal screw $\hat{\$}_{rt,i}$. Moreover, λ_i represents the pitch of the reciprocal screw $\hat{\$}_{rt,i}$. Using Eqs. (28), (29) and (30), we concluded that:

$$s_{rt,i} = \frac{a_i}{\sqrt{a_i^2 + b_i^2}}\begin{bmatrix} \sin(\alpha_i)\cos(\beta_i) \\ -\sin(\beta_i) \\ \cos(\alpha_i)\cos(\beta_i) \end{bmatrix} + \frac{b_i}{\sqrt{a_i^2 + b_i^2}}\begin{bmatrix} -\cos(\alpha_i) \\ 0 \\ \sin(\alpha_i) \end{bmatrix}. \tag{31}$$

The reciprocal screw $\hat{\$}_{rt,i}$ must be a reciprocal with the prismatic joint screw $\hat{\$}_{1,i}$ provided in Eq. (15). This condition can be written as:

$$s_{rt,i}^T \cdot s_{1,i} = 0. \tag{32}$$

The previous equation will lead to:

$$\frac{a_i}{\sqrt{a_i^2 + b_i^2}}\cos(\alpha_i)\cos(\beta_i) + \frac{b_i}{\sqrt{a_i^2 + b_i^2}}\sin(\alpha_i) = 0. \tag{33}$$

Assume b_i with any random value, then find a_i:

$$a_i = \frac{-b_i\sin(\alpha_i)}{\cos(\alpha_i)\cos(\beta_i)}\ . \tag{34}$$

At the same configuration, changing b_i leads to a change in a_i, but $\hat{S}_{rt,i}$ and λ_i are fixed for this configuration and expressed as:

$$\hat{\$}_{rt,i} = \begin{bmatrix} \dfrac{-1}{\cos(\alpha_i)\sqrt{\frac{\cos^2(\alpha_i)\cos^2(\beta_i) - \cos^2(\alpha_i) + 1}{\cos^2(\alpha_i)\cos^2(\beta_i)}}} \\ \dfrac{\sin(\alpha_i)\sin(\beta_i)}{\cos(\alpha_i)\cos(\beta_i)\sqrt{\frac{\sin^2(\alpha_i)}{\cos^2(\alpha_i)\cos^2(\beta_i)} + 1}} \\ 0 \\ \dfrac{-\sin(\alpha_i)[d_i\sin(\beta_i + \gamma_i)\sin(\beta_i) + L_i\cos(\alpha_i)\cos(\beta_i)\cos(\gamma_i)]}{\sin(\beta_i + \gamma_i)\cos(\alpha_i)\cos(\beta_i)\sqrt{\frac{\sin^2(\alpha_i)}{\cos^2(\alpha_i)\cos^2(\beta_i)} + 1}} \\ \dfrac{-d_i}{\cos(\alpha_i)\sqrt{\frac{\cos^2(\alpha_i)\cos^2(\beta_i) - \cos^2(\alpha_i) + 1}{\cos^2(\alpha_i)\cos^2(\beta_i)}}} \\ \dfrac{-[L_i\cos^2(\alpha_i)\cos(\beta_i)\cos(\gamma_i) - \psi\sin(\beta_i + \gamma_i)\sin(\alpha_i)\sin(\beta_i)]}{\cos(\beta_i + \gamma_i)\cos(\alpha_i)\cos(\beta_i)\sqrt{\frac{\sin^2(\alpha_i)}{\cos^2(\alpha_i)\cos^2(\beta_i)} + 1}} \end{bmatrix}, \tag{35}$$

$$\lambda_i = \frac{L_i\cos(\alpha_i)\cos^2(\beta_i)\cos(\gamma_i)\sin(\alpha_i)}{\sin(\beta_i + \gamma_i)[\cos^2(\alpha_i)\cos^2(\beta_i) - \cos^2(\alpha_i) + 1]}\ . \tag{36}$$

You should remember that we use $\psi = R$ for the first limb ($i = 1$) and $\psi = -R$ for the third limb ($i = 3$). It is clear that the pitch of the reciprocal screw λ_i depends on the configuration as it is a function of the angles of the two universal joints.

It is worth mentioning that there is a special case when the two planes (each plane contains the two axes of a universal joint) are parallel to each other as shown in Fig. 5. In this case, there is not any intersection line between the two planes, hence $\hat{\$}_{r2,i}$ could not be obtained. The case of parallel planes occurs when $\beta_i + \gamma_i = 0$ *or* π. So,

$$n_{1,i} = n_{2,i} = \begin{bmatrix} -\sin(\alpha_i) \\ 0 \\ -\cos(\alpha_i) \end{bmatrix}. \tag{37}$$

In this case, while the actuator is locked, the reciprocal screws for this limb, which is reciprocal to all the passive joint screws form a 2-system. One screw, $\hat{\$}_{r1,i}$, can be readily identified as a zero pitch screw along the line connecting the two centers of the two universal joints. The closed form of $\hat{\$}_{r1,i}$ is presented in Eq. (20). The second reciprocal screw, $\hat{\$}_{r2,i}$, which is also reciprocal to all the passive joint screws can be readily identified as an infinity pitch

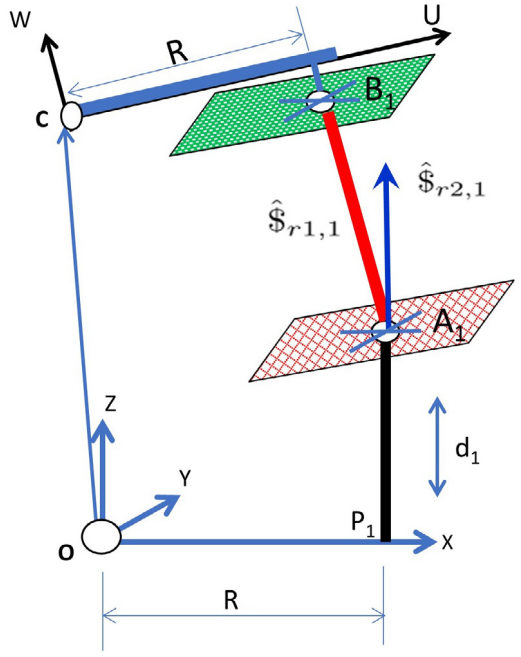

Fig. 5. Special case for reciprocal screws of first limb PUU.

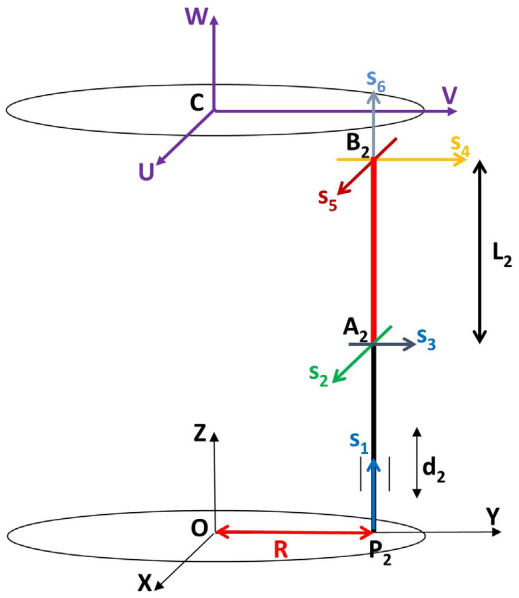

Fig. 6. Schematic representation of second chain PUS.

screw along the normal line of the two planes as shown in Fig. 5. The closed form of $\hat{\$}_{r2,i}$ is expressed as:

$$\hat{\$}_{r2,i} = \begin{bmatrix} 0 \\ 0 \\ 0 \\ -\sin(\alpha_i) \\ 0 \\ -\cos(\alpha_i) \end{bmatrix}. \tag{38}$$

Without locking the prismatic joint, the reciprocal screws for this limb form a 1-system which is a screw that is reciprocal to all the joint screws of the ith limb. This reciprocal screw, $\hat{\$}_{rt,i}$, is equal to $\hat{\$}_{r2,i}$ as presented in Eq. (38).

4.2. Second and fourth limbs

Each limb of second and fourth limbs connects the fixed base to the moving platform by a prismatic joint followed by a universal joint and another spherical joint (PUS). The prismatic joint is driven by a linear actuator. Fig. 6 shows the schematic representation of the second limb and its joints' axes.

The position vector of the center of the spherical joint B_i ($i = 2, 4$ for second and fourth limbs, respectively) with respect to the reference frame O-XYZ can be described as:

$$B_i = A_i + rot_x(\alpha_i) \cdot rot_y(\beta_i) \cdot \begin{bmatrix} 0 \\ 0 \\ L_i \end{bmatrix} = \begin{bmatrix} L_i \sin(\beta_i) \\ \psi - L_i \sin(\alpha_i)\cos(\beta_i) \\ d_i + L_i \cos(\alpha_i)\cos(\beta_i) \end{bmatrix}, \tag{39}$$

where α_i and β_i are the two angles of the first universal joint in the ith limb ($i = 2, 4$ for second and fourth limbs, respectively). For easy flow of equations, we use $\psi = R$ for the second limb ($i = 2$) and $\psi = -R$ for the fourth limb ($i = 4$). Each limb may be considered as a serial limb consisting of 6 joints with 1 DOF. Therefore, the connectivity of each limb is equal to 6. Let $s_{j,i}$ be a unit vector along the jth joint axis of the ith limb (*for* $i = 2, 4$; and $j = 1, 2, \ldots, 6$). Now, we will calculate the unit vector associated with all joints' axes in the second and fourth limbs. The fixed frame O-XYZ is chosen to be the reference frame at which all the screws are expressed.

$$s_{1,i} = \begin{bmatrix} 0 \\ 0 \\ 1 \end{bmatrix}, \qquad s_{2,i} = \begin{bmatrix} 1 \\ 0 \\ 0 \end{bmatrix}, \tag{40}$$

$$s_{3,i} = rot_x(\alpha_i) \cdot \begin{bmatrix} 0 \\ 1 \\ 0 \end{bmatrix} = \begin{bmatrix} 0 \\ \cos(\alpha_i) \\ \sin(\alpha_i) \end{bmatrix}, \tag{41}$$

$$s_{4,i} = rot_x(\alpha_i) \cdot rot_y(\beta_i) \cdot \begin{bmatrix} 0 \\ 1 \\ 0 \end{bmatrix} = \begin{bmatrix} 0 \\ \cos(\alpha_i) \\ \sin(\alpha_i) \end{bmatrix}, \tag{42}$$

$$s_{5,i} = rot_x(\alpha_i) \cdot rot_y(\beta_i) \cdot rot_y(\gamma_i) \cdot \begin{bmatrix} 1 \\ 0 \\ 0 \end{bmatrix} = \begin{bmatrix} \cos(\beta_i + \gamma_i) \\ \sin(\alpha_i)\sin(\beta_i + \gamma_i) \\ -\cos(\alpha_i)\sin(\beta_i + \gamma_i) \end{bmatrix}. \tag{43}$$

$$s_{6,i} = rot_x(\alpha_i) \cdot rot_y(\beta_i) \cdot rot_y(\gamma_i) \cdot rot_x(\delta_i) \cdot \begin{bmatrix} 0 \\ 0 \\ 1 \end{bmatrix} = \begin{bmatrix} \cos(\delta_i)\sin(\beta_i + \gamma_i) \\ -\sin(\delta_i)\cos(\alpha_i) - \cos(\delta_i)\sin(\alpha_i)[\cos(\beta_i)\cos(\gamma_i) - \sin(\beta_i)\sin(\gamma_i)] \\ -\sin(\delta_i)\sin(\alpha_i) + \cos(\delta_i)\cos(\alpha_i)[\cos(\beta_i)\cos(\gamma_i) - \sin(\beta_i)\sin(\gamma_i)] \end{bmatrix}, \tag{44}$$

where γ_i, δ_i, and σ_i are the three angles of the spherical joint in the ith limb.

With the actuator locked, the connectivity of each limb is equal to 5. Therefore, the reciprocal screws for each limb of second and fourth limbs form a 1-system. This screw, $\hat{\$}_{r1,i}$, which is reciprocal to all the passive joint screws of the ith limb can be readily identified as a zero pitch screw along the line passing through the two centers of the universal and spherical joints. A unit vector $s_{r1,i}$ along the axis of the reciprocal screw $\hat{\$}_{r1,i}$ can be identified from:

$$s_{r1,i} = rot_x(\alpha_i) \cdot rot_y(\beta_i) \cdot \begin{bmatrix} 0 \\ 0 \\ 1 \end{bmatrix} = \begin{bmatrix} \sin(\beta_i) \\ -\sin(\alpha_i)\cos(\beta_i) \\ \cos(\alpha_i)\cos(\beta_i) \end{bmatrix}. \tag{45}$$

Moreover, $s_{r01,i}$, which is a vector from the origin of the reference frame to a point existing on the line passing through the center of the universal and spherical joints, can be easily calculated from $s_{r01,i} = A_i$. Knowing $s_{r1,i}$ and $s_{r01,i}$, we can identify a zero pitch screw, $\hat{\$}_{r1,i}$, according to:

$$\hat{\$}_{r1,i} = \begin{bmatrix} \sin(\beta_i) \\ -\sin(\alpha_i)\cos(\beta_i) \\ \cos(\alpha_i)\cos(\beta_i) \\ \psi\cos(\alpha_i)\cos(\beta_i) + d_i\sin(\alpha_i)\cos(\beta_i) \\ d_i\sin(\beta_i) \\ -\psi\sin(\beta_i) \end{bmatrix}. \tag{46}$$

Without locking the active prismatic joint, the connectivity is equal to 6 for each limb of the second and fourth limbs. Hence, no screw can be identified to be reciprocal to all the joint screws of the ith limb.

5. Singular configurations of parallel surgical manipulator (2-PUU_2-PUS)

5.1. Constraint singularities

Constraint singularities arise when the limbs of (2-PUU_2-PUS) parallel manipulator lose their ability to constrain the movable platform to move with the intended motion. It can be shown that the Jacobian of constraints J_c is a 2×6 matrix. A unit wrench of constraints imposed by the joints of a limb will be represented as a row in the Jacobian of constraint matrix, J_c. To properly constrain the moving platform to 4-DOF motion, the rank of J_c should be equal to 2. The Jacobian of constraints J_c of (2-PUU_2-PUS) parallel surgical manipulator is indicated as:

$$J_c = \begin{bmatrix} \hat{\$}_{rt,1}^T \\ \hat{\$}_{rt,3}^T \end{bmatrix}, \tag{47}$$

where the two rows of J_c can be obtained from Eq. (35). Constraint singularities arise when the Jacobian of constraints (J_c) loses its rank, i.e. the rank of J_c is less than 2. These singularities will occur when $\hat{\$}_{rt,1}^T$ and $\hat{\$}_{rt,3}^T$ become linearly dependent (LD).

In finding the whole workspace and the singular configurations, we take into consideration all the mechanical limits of the prismatic and universal joints. Regarding the prismatic joint, we take into account the length of its stroke. As stated by the manufacturers of the small-scale universal joint of the (MAAS 1.0) type [22], the angle limitation is $\pm 90°$ for one angle and $\pm 30°$ for the other angle, i.e. the sum of the two angles is less than or equal to 120°.

The following states present the conditions for constraint singularities.

(1) When $(\alpha_1 = \alpha_3 = 0)\,\&\,(\beta_1 = \beta_3 = \beta)\,\&\,(\gamma_1 = \gamma_3 = \gamma)\,\&\,(d_1 = d_3 = d)$,

$$\hat{\$}_{rt,1} = \hat{\$}_{rt,3} = \begin{bmatrix} -1 \\ 0 \\ 0 \\ 0 \\ -d \\ -L\cos(\gamma)/\sin(\beta+\gamma) \end{bmatrix}, \tag{48}$$

where β, γ and d are random values. Also, at this state, the pitches of the two reciprocal screws will be $\lambda_1 = \lambda_3 = 0$. A search for points inside the workspace to satisfy this condition is achieved considering the mechanical limitations of the joints. It is found that all the points in the YZ plane can satisfy this condition as shown in Fig. 7. Hence, constraint singularity configurations occur when the center of the movable platform lies on the YZ orthogonal plane.

(2) When $(\alpha_1 = \alpha_3 = \alpha)\,\&\,(\beta_1 = \beta_3 = 0)\,\&\,(\gamma_1 = \gamma_3 = \gamma)\,\&\,(d_1 = d_3 = d)$,

$$\hat{\$}_{rt,1} = \hat{\$}_{rt,3} = \begin{bmatrix} -1 \\ 0 \\ 0 \\ \dfrac{-L\sin(\alpha)\cos(\gamma)}{\sin(\gamma)\sqrt{\frac{1}{\cos^2(\alpha)}}} \\ -d \\ \dfrac{-L\cos(\alpha)\cos(\gamma)}{\sin(\gamma)\sqrt{\frac{1}{\cos^2(\alpha)}}} \end{bmatrix}, \tag{49}$$

where α, γ and d are random values. Also, at this state, the pitches of the two reciprocal screws will be $\lambda_1 = \lambda_3 = \frac{-L\cos(\alpha)\sin(\alpha)\cos(\gamma)}{\sin(\gamma)}$. Another search for points inside the workspace to satisfy this condition is achieved considering the mechanical limitations of the joints. It is found that all the points in the XZ plane can satisfy this condition as shown in Fig. 8. Hence, constraint singularity configurations occur when the center of the movable platform lies on the XZ orthogonal plane.

(3) When $(\alpha_1 = \alpha_3 = 0)\,\&\,(\beta_1 = \beta_3 = 0)\,\&\,(\gamma_1 = \gamma_3 = \gamma)\,\&\,(d_1 = d_3 = d)$,

$$\hat{\$}_{rt,1} = \hat{\$}_{rt,3} = \begin{bmatrix} -1 \\ 0 \\ 0 \\ 0 \\ -d \\ \dfrac{-L\cos(\gamma)}{\sin(\gamma)} \end{bmatrix}, \tag{50}$$

where γ and d are any random values. Also, at this state, the pitches of the two reciprocal screws will be $\lambda_1 = \lambda_3 = 0$. A Search for points inside the workspace to satisfy this condition is achieved considering the mechanical limitations of the joints. It is found that all the points located at the intersecting line between XZ plane and YZ plane can satisfy this condition as shown in Fig. 9. Hence, constraint singularity configurations occur when the center of the movable platform lies on the orthogonal Z-axis.

(4) When $(\alpha_1 = \alpha_3 = \alpha)\,\&\,(\beta_1 = \beta_3 = \beta)\,\&\,(\gamma_1 = \gamma_3 = \gamma)\,\&\,(d_1 = d_3 = d)\,\&\,(\beta + \gamma = 0)$,

where α, β, γ and d are random values. After searching for points inside the workspace and satisfying this condition, considering the mechanical limitations of the joints, it is found that this condition will not occur unless $d_1 = d_2 = d_3 = d_4$. Therefore, this state can be avoided by avoiding the equality of prismatic joints' values in the control law.

From the above four states, we discovered that singularity configurations occur when the center of the movable platform lies on two orthogonal planes. These planes are parallel to the axes of the prismatic joints, and each plane contains the axes of two opposite prismatic joints and passes through the center of the fixed base. These orthogonal planes divide the workspace into four equal parts as shown in Fig. 10. Thus, the singularity-free workspace is one-fourth of the original workspace.

5.2. Architecture singularities

Architecture singularities point out the conditions for which the actuators cannot control the linear velocity of the movable platform. Writing Eq. (4) once for each limb produces four equations, which can be written in matrix form as Eq. (5) where:

$$J_x = \begin{bmatrix} \hat{\$}_{r1,1}^T \\ \hat{\$}_{r1,2}^T \\ \hat{\$}_{r1,3}^T \\ \hat{\$}_{r1,4}^T \end{bmatrix}, \tag{51}$$

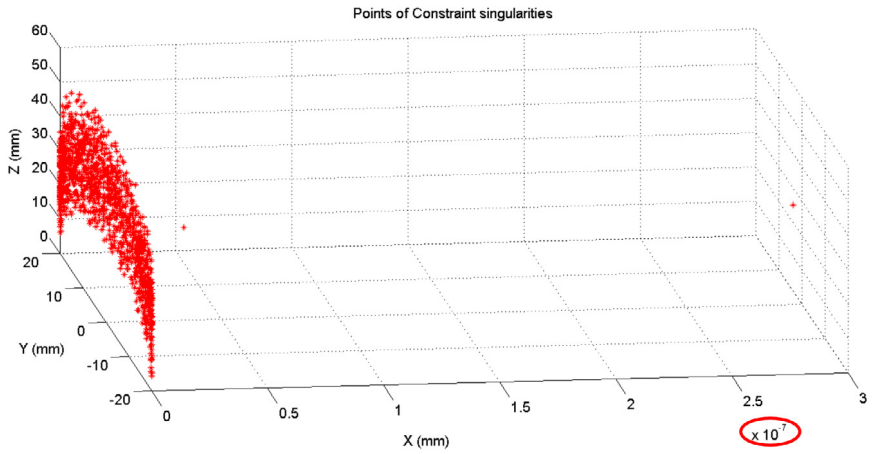

Fig. 7. Points that satisfy first constraint singularities condition.

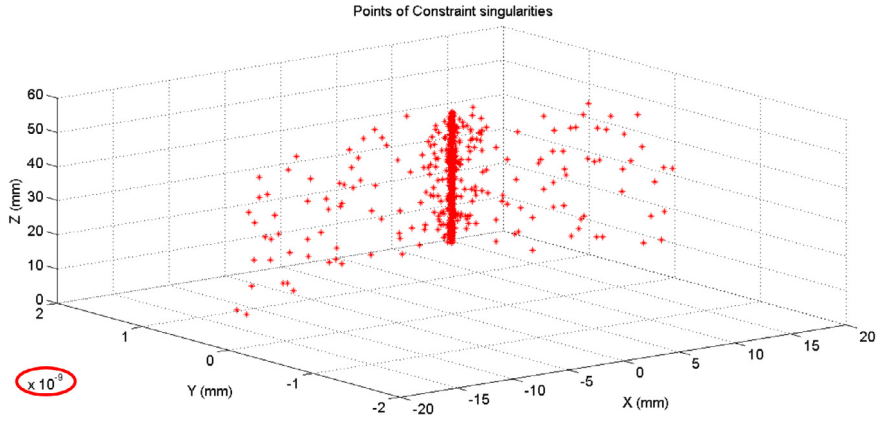

Fig. 8. Points that satisfy second constraint singularities condition.

$$J_q = \begin{bmatrix} \hat{\$}_{r1,1}^T \cdot \hat{\$}_{1,1} & 0 & 0 & 0 \\ 0 & \hat{\$}_{r1,2}^T \cdot \hat{\$}_{1,2} & 0 & 0 \\ 0 & 0 & \hat{\$}_{r1,3}^T \cdot \hat{\$}_{1,3} & 0 \\ 0 & 0 & 0 & \hat{\$}_{r1,4}^T \cdot \hat{\$}_{1,4} \end{bmatrix}. \quad (52)$$

Note that J_x is a 4 $\times$ 6 matrix and J_q is a 4 $\times$ 4 diagonal matrix. Multiplying both sides of Eq. (5) by J_q^{-1} yields Eq. (6) where:

$$J_a = \begin{bmatrix} \hat{\$}_{r1,1}^T / (\hat{\$}_{r1,1}^T \cdot \hat{\$}_{1,1}) \\ \hat{\$}_{r1,2}^T / (\hat{\$}_{r1,2}^T \cdot \hat{\$}_{1,2}) \\ \hat{\$}_{r1,3}^T / (\hat{\$}_{r1,3}^T \cdot \hat{\$}_{1,3}) \\ \hat{\$}_{r1,4}^T / (\hat{\$}_{r1,4}^T \cdot \hat{\$}_{1,4}) \end{bmatrix}. \quad (53)$$

J_a is a 4 $\times$ 6 Jacobian matrix. The rank of J_a should be equal to 4. Actuation singularities occur when $\det(J) = 0$ but J_c has a full rank of 2. These singularities will occur when two or more of the reciprocal screws from $\hat{\$}_{r1,1}$, $\hat{\$}_{r1,2}$, $\hat{\$}_{r1,3}$ and $\hat{\$}_{r1,4}$ become linearly dependent (LD). The following states present the conditions for actuation singularities.

(1) When $(\alpha_1 = \alpha_3 = \pi/2) \,\&\, (\beta_1 = \beta_3 = 0) \,\&\, (d_1 = d_3 = d)$, $\hat{\$}_{r1,1} = \hat{\$}_{r1,3} = \begin{bmatrix} 1, & 0, & 0, & 0, & d, & 0 \end{bmatrix}^T$.

(2) When $(\alpha_2 = \alpha_4 = \pi/2) \,\&\, (\beta_2 = \beta_4 = 0) \,\&\, (d_2 = d_4 = d)$, $\hat{\$}_{r1,2} = \hat{\$}_{r1,4} = \begin{bmatrix} 0, & -1, & 0, & d, & 0, & 0 \end{bmatrix}^T$.

where d is any random value. Referring to Fig. 3, it is easy for the reader to imagine the state when A_1B_1 is perpendicular to P_1A_1, which represents that $(\alpha_1 = \pi/2)$. From the above two states, we discovered that architecture singularity will be occurring when each connecting rod A_iB_i in the two opposite limbs of the manipulator is perpendicular to the prismatic joint axis P_iA_i (*for* i = 1,2,3,4). So, the bending angle of the manipulator could not be greater than $\pm 90°$ in any direction, which is acceptable in surgical applications.

5.3. ADAMS software and experimental verification

In order to prove the correctness of the approach, some experiments have been done as shown in the videos at the following three links:

a-https://www.dropbox.com/s/kp2a1ulc1xwq6so/Media1.avi?dl=0

b-https://www.dropbox.com/s/yaeopun75fs5kei/Media2.mp4?dl=0

c-https://www.dropbox.com/s/0fvqpbsu2ial9ix/Media3.mp4?dl=0.

The virtual prototype of the 2-PUU_2-PUS parallel manipulator is constructed using ADAMS software to check the correctness of the proposed approach. The first video shows that the movable platform of the manipulator is moving, although the prismatic links are fixed in the same position. Therefore, this video illustrates that the movable platform could not resist any force in this configuration as the gravitational force makes its movement to the movable platform. This configuration illustrates the concept of constraint

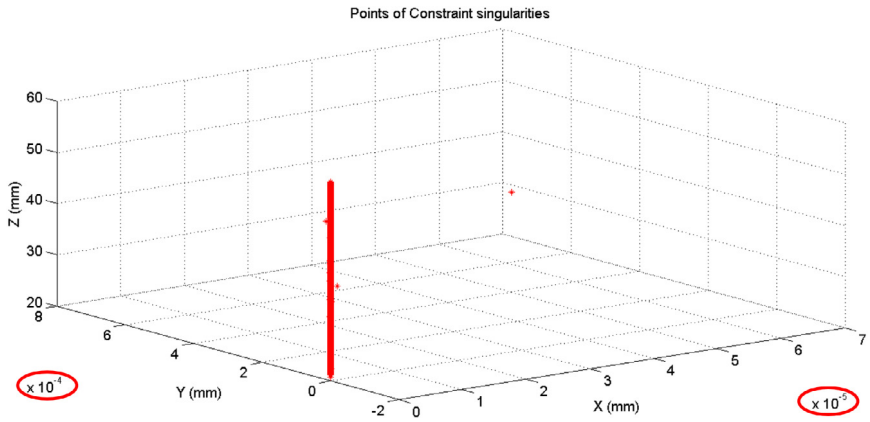

Fig. 9. Points that satisfy third constraint singularities condition.

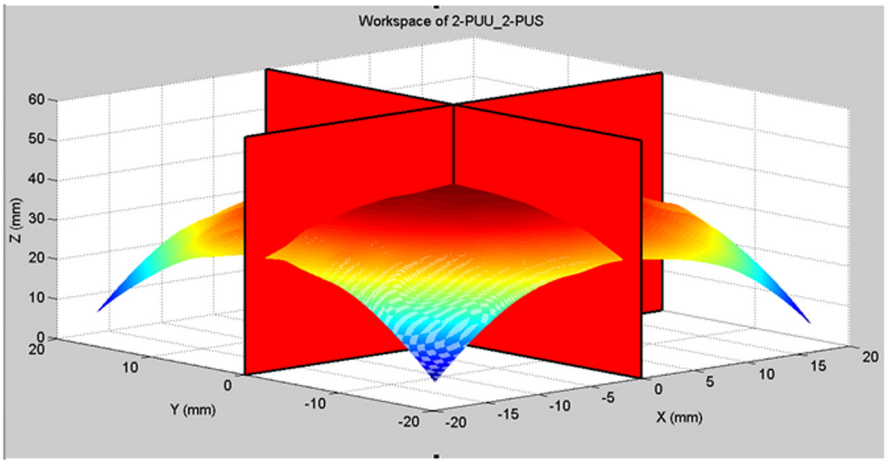

Fig. 10. Workspace of 2-PUU_2-PUS with singular planes.

singularity. Similarly, the second video shows a singular configuration of the real manipulator in which the movable platform of the manipulator is moving although the prismatic links are fixed.

Additionally, the third video shows a practical implementation of the whole teleoperated system in which the PHANTOM-Omni haptic device is used as the master robot and the 2-PUU_2-PUS parallel manipulator as the slave one. A singular configuration appeared at the time 01:04 in which the movable platform of the manipulator could not resist any force (gravitational force moves the movable platform although the prismatic joints are fixed). The 2-PUU_2-PUS parallel manipulator will not be able to cut or do its task at the singular configurations.

6. Conclusions

Geometrical/Analytical approach for reciprocal screw-based singularity analysis is proposed to facilitate the singularity analysis of parallel manipulators with h-pitch wrench systems. This proposed algorithm is used to find all singular configurations inside the workspace of 2-PUU_2-PUS, which has h-pitch reciprocal screws. The discovered singularity configurations of (2-PUU_2-PUS) occur when the center of the movable platform lies on two orthogonal planes. These planes are parallel to the axes of the prismatic joints, and each plane contains the axes of two opposite prismatic joints and passes through the center of the fixed base. These orthogonal planes divide the workspace into four equal parts. Thus, the singularity-free workspace is one-fourth the original workspace. ADAMS software and experiments have been used for algorithm verification. They prove the correctness of the approach. As a future work, design modifications of the proposed manipulator are needed to move across the singularity planes and retain the original workspace.

Acknowledgments

The first author is supported by a scholarship from the Mission Department, Ministry of Higher Education of the Government of Egypt which is gratefully acknowledged. Our sincere thanks to Egypt-Japan University of Science and Technology (E-JUST) for guidance and support.

References

[1] Koji Ikuta, Keiichi Yamamoto, Keiji Sasaki, Development of remote microsurgery robot and new surgical procedure for deep and narrow space, in: IEEE International Conference on Robotics and Automation, 2003. Proceedings, Vol. 1, ICRA'03, IEEE, 2003.

[2] G. Guthart, J. Salisbury, The intuitive telesurgery system: Overview and application, in: Proc. IEEE Int. Conf. Robot. Autom. San Francisco, CA, 2000, pp. 618–621.

[3] P. Berkelman, J. Ma, A compact modular teleoperated robotic system for laparoscopic surgery, Int. J. Robot. Res. (2009) 1198–1215.

[4] Ulrich Hagn, et al., DLR MiroSurge: a versatile system for research in endoscopic telesurgery, Int. J. Comput. Assist. Radiol. Surg. 5 (2) (2010) 183–193.

[5] Nabil Simaan, Russell Taylor, Paul Flint, A dexterous system for laryngeal surgery, in: 2004 IEEE International Conference on Robotics and Automation, 2004. Proceedings, Vol. 1, ICRA'04, IEEE, 2004.

[6] Kai Xu, Nabil Simaan, An investigation of the intrinsic force sensing capabilities of continuum robots, IEEE Trans. Robot. 24 (3) (2008) 576–587.
[7] Chin, Wei Jian, Carl A. Nelson, Chi Min Seow, Articulated Mechanism Design and Kinematics for Natural Orifice Translumenal Endoscopic Surgery Robot. Diss, University of Nebraska-Lincoln, 2011.
[8] C. Vaida, et al., Orientation module for surgical instruments—a systematical approach, Meccanica 48 (1) (2013) 145–158.
[9] Van Meer, Frederick, et al., A disposable plastic compact wrist for smart minimally invasive surgical tools, in: 2005 IEEE/RSJ International Conference on Intelligent Robots and Systems, 2005, (IROS 2005), IEEE, 2005.
[10] Doina Pisla, et al., An active hybrid parallel robot for minimally invasive surgery, Robot. Comput.-Integr. Manuf. 29 (4) (2013) 203–221.
[11] T.K. Tanev, et al. Elastostatic model of a new hybrid minimally-invasive-surgery robot, in: The 14th IFToMM World Congress, Taipei, Taiwan, 2015.
[12] Khalil Ibrahim, et al., Development of a new 4-DOF endoscopic parallel manipulator based on screw theory for laparoscopic surgery, Mechatronics 28 (2015) 4–17.
[13] Horin, Patricia Ben, Moshe Shoham, A class of parallel robots practically free of parallel singularities, J. Mech. Des. 130 (5) (2008) 052303.
[14] Masouleh, Mehdi Tale, Clment Gosselin, Singularity analysis of 5-RPUR parallel mechanisms (3T2R), Int. J. Adv. Manuf. Technol. 57 (9–12) (2011) 1107–1121.
[15] Patricia Ben-Horin, Moshe Shoham, Application of GrassmannCayley algebra to geometrical interpretation of parallel robot singularities, Int. J. Robot. Res. 28 (1) (2009) 127–141.
[16] Leila Notash, Uncertainty configurations of parallel manipulators, Mech. Mach. Theory 33 (1) (1998) 123–138.
[17] Dash, Anjan Kumar, et al., Instantaneous kinematics and singularity analysis of three-legged parallel manipulators, Robotica 22 (02) (2004) 189–203.
[18] Jean-Pierre Merlet, Singular configurations of parallel manipulators and Grassmann geometry, Int. J. Robot. Res. 8 (5) (1989) 45–56.
[19] D. Zlatanov, R.G. Fenton, B. Benhabib, A unifying framework for classification and interpretation of mechanism singularities, J. Mech. Des. 117 (4) (1995) 566–572.
[20] Sameer A. Joshi, Lung-Wen Tsai, Jacobian analysis of limited-DOF parallel manipulators, in: ASME 2002 International Design Engineering Technical Conferences and Computers and Information in Engineering Conference, American Society of Mechanical Engineers, 2002.
[21] Lung-Wen Tsai, Robot Analysis: The Mechanics of Serial and Parallel Manipulators, John Wiley & Sons, 1999.
[22] http://www.miyoshikikai.co.jp/en/ [Last accessed 07.06.17].

Alaa Khalifa received the B.Sc. degree in industrial electronics and control engineering from Faculty of Electronic Engineering, Menoufia University, Al Menoufia, Egypt, in 2010; and the M.Sc. degree in mechatronics and robotics engineering from Egypt-Japan University of Science and Technology, New Borg El Arab, Alexandria, Egypt, in 2015. Then, he worked toward the Ph.D. degree from Feb 2015 till now. He worked as exchange researcher at Waseda University, Tokyo, Japan, for six months. His current research focuses on Surgical Manipulators, Teleoperation systems, and Control system design.

Mohamed Fanni received the B.E. degree in mechanical engineering from the Faculty of Engineering, Cairo University, Giza, Egypt, in 1981; the M.Sc. degree in mechanical engineering from Mansoura University, Mansoura, Egypt, in 1986; and the Ph.D. degree in engineering from Karlsruhe University, Karlsruhe, Germany, in 1993. He is an Associate Professor with the Egypt-Japan University of Science and Technology, New Borg El Arab, Egypt, on leave from the Production Engineering and Mechanical Design Department, Faculty of Engineering, Mansoura University. His major research interests include robotics engineering, automatic control, and mechanical design. His current research focuses on design and control of mechatronic systems, surgical manipulators, and flying/walking robots.

Abdelfatah Mohamed has received the Ph.D. degree from University of Maryland, College park, USA in 1990. Since 1990 he has been an Assistant Professor with the Dept. of Electrical Engineering, Assiut University, Egypt. He became an Associate Professor in 1995, and Professor in 2000. From September 1990 to August 1993, he has been a Postdoctoral Fellow at the Dept. of Mechanical Engineering, University of Texas, Austin USA. From April 1996 to April 1997. He has been a visiting Professor at the Dept. of Electrical Engineering, Kanazawa University, Japan. From September 2010 to March 2012 He has been the Head, Dept. of Electrical Engineering, Assiut University, and became the Dean of Faculty of Engineering, Assiut University on March 2012. Currently He is the head of the Dept. of Mechatronics and Robotics Engineering, Egypt-Japan University of Science & Technology. His research interest lies in Robust and Intelligent control, Magnetic Bearing systems, Robotics, Industrial drives. Dr. Mohamed is a senior IEEE member.